Journal of Hazardous Materials 186 (2011) 575–582

Contents lists available at ScienceDirect

Journal of Hazardous Materials

journal homepage: www.elsevier.com/locate/jhazmat

Efficient removal of chromate and arsenate from individual and mixed system by malachite nanoparticles

Jiban Saikia [a], Bedabrata Saha [b], Gopal Das [a,b,*]

[a] Department of Chemistry, Indian Institute of Technology Guwahati, Assam 781039, India
[b] Centre for the Environment, Indian Institute of Technology Guwahati, Assam 781039, India

ARTICLE INFO

Article history:
Received 23 September 2010
Received in revised form 8 November 2010
Accepted 9 November 2010
Available online 13 November 2010

Keywords:
Malachite nanoparticles
Competitive adsorption
Chromate
Arsenate
Adsorption selectivity

ABSTRACT

Malachite nanoparticles of 100–150 nm have been efficiently and for the first time used as an adsorbent for the removal of toxic arsenate and chromate. We report a high adsorption capacity for chromate and arsenate on malachite nanoparticle from both individual and mixed solution in pH ~4–5. However, the adsorption efficiency decreases with the increase of solution pH. Batch studies revealed that initial pH, temperature, malachite nanoparticles dose and initial concentration of chromate and arsenate were important parameters for the adsorption process. Thermodynamic analysis showed that adsorption of chromate and arsenate on malachite nanoparticles is endothermic and spontaneous. The adsorption of these anions has also been investigated quantitatively with the help of adsorption kinetics, isotherm, and selectivity coefficient (K) analysis. The adsorption data for both chromate and arsenate were fitted well in Langmuir isotherm and preferentially followed the second order kinetics. The binding affinity of chromate is found to be slightly higher than arsenate in a competitive adsorption process which leads to the comparatively higher adsorption of chromate on malachite nanoparticles surface.

1. Introduction

The recent environmental issues are receiving increasing attention for being contaminated by toxic elements such as chromium and arsenic due to their potentially hazardous risk to public health and the environment. Arsenate and chromate are toxic anionic pollutants that contaminate the water system and enter the food chain causing fatal disease in human [1–4]. These toxic pollutants are introduced into the environment from a variety of processes such as, mineral weathering, mining, industrial applications including leather tanning, textile dyeing, metal finishing, electroplating, inorganic chemicals production [5,6]. Hexavalent chromium usually exists in wastewater as oxyanions such as chromate (CrO_4^{2-}) and dichromate ($Cr_2O_7^{2-}$) which are mostly toxic, carcinogenic and mutagenic and does not precipitate easily using conventional precipitation methods [7,8]. Similarly, the common forms of arsenate predominantly present are $H_2AsO_4^-$, $HAsO_4^{2-}$and AsO_4^{3-} [9] in oxygen rich aerobic waste sources [10] are capable of imposing several health hazards in terms of various skin, lung, and kidney cancer as well as pigmentation changes, neurological disorders, muscular weakness, etc. [11–13]. Therefore, the removal of these pollutants from the contaminated waste sources is critically important for the protection of human health and sustainable environment.

Numerous methods have been developed for the removal of such pollutants in wastewater, including adsorption, electrochemical precipitation, ion exchange, membrane ultra-filtration, reverse osmosis and reduction [5,6,14,15]. Emerging as one of the most promising techniques for removal of pollutants from industrial wastewaters, adsorption technology has been employed widely [16] and established as an effective method in remediation technologies. Adsorption, when combined with appropriate desorption step, can also solves the problem of sludge disposal [17], which is a major concern in precipitation method.

Now a days, nanoparticles are in high demand in environmental remediation technologies for their high surface to volume ratio. As discussed above, a nano-structured materials having positive charge on its surface can be effective for adsorbing the anionic pollutants from waste sources. In this regard, malachite nanoparticles [18], a basic hydrophilic surface, can be a good choice for removal of chromate and arsenate. Malachite or basic copper carbonate is a naturally occurring secondary copper mineral with the composition of $Cu_2(OH)_2CO_3$. Previous studies have reported that the malachite nanoparticles have the $-CO_3$ and –OH groups on the surface [18,19], having a pH_{pzc} of ~7.5. Therefore, the malachite nanoparticle surface would be positively charged in the broad pH

* Corresponding author at: Department of Chemistry, Indian Institute of Technology Guwahati, North Guwahati, Guwahati, Assam 781039, India.
Tel.: +91 361 258 2313; fax: +91 361 258 2349.
E-mail address: gdas@iitg.ernet.in (G. Das).

0304-3894/$ – see front matter © 2010 Elsevier B.V. All rights reserved.
doi:10.1016/j.jhazmat.2010.11.036

range upto ~7.5, which in turn can be a potential surface for adsorption of anionic pollutants such as chromate and arsenate.

In this article, we demonstrate the adsorption behaviour of two anionic pollutants such as, chromate and arsenate on a new basic hydrophilic nanoparticle surface. Malachite nanoparticles with an average size of 100–150 nm have been prepared and characterized previously [18]. For the first time, malachite nanoparticles have been used for the adsorption studies of anionic pollutants such as chromate and arsenate. Herein, we report higher and simultaneous removal of both chromate and arsenate from single as well as binary system. Influence of other variable parameters likely, pH, temperature and concentration was studied in detail. Detail adsorption kinetics, isotherm studies and thermodynamic analysis have also been for both cases.

2. Experimental

2.1. Materials

Stock solutions of 500 mg L^{-1} of chromate and arsenate were prepared from $K_2Cr_2O_7$ and $Na_2HAsO_4{\cdot}7H_2O$ of analytical grade procured from Merck India. From the stock standard solutions, anion solutions of the desired concentrations for experimentation were prepared by appropriate dilution with Milli-Q water (18.2 MΩ) as required.

2.2. Preparation of malachite nanoparticles and adsorption studies

Malachite nanoparticles with an average size of 100–150 nm have been synthesized and characterized as described previously [18]. Briefly, 8 mM of $CuSO_4{\cdot}5H_2O$ solution was stirred well with 4 mM aqueous solution of SDS; 10 mM Na_2CO_3 solution was then added drop wise with constant stirring at room temperature. The green suspension formed, was separated by centrifugation, and was subsequently washed with alcohol and Milli-Q water prior to use. Synthesized malachite nanoparticles were previously characterized by transmission electron micrograph (TEM), thermogravimetric analysis (TGA), FT-IR spectroscopy, and powder X-ray diffraction (PXRD). The surface area and the surface charge of malachite nanoparticles were analyzed by BET-isotherm analysis and ζ-potential measurement, respectively [18].

Adsorption experiments were conducted in batch technique to obtain kinetic and equilibrium data. Different initial concentrations of chromate and arsenate were stirred with defined 5 g L^{-1} of malachite nanoparticles separately. Solution pH of the adsorption experiments was varied (by 0.1 M HCl and NaOH) from 4.0 to 9.0 to check the adsorption efficiency of malachite nanoparticles for both chromate and arsenate. Kinetics experiments were carried out at different time interval by withdrawing the aliquot of supernatant from the adsorption mixture until steady state reaches. The sample withdrawn from solution at regular time interval was immediately centrifuged in 15,000 rpm for 10 min to stop further reaction. The supernatant was collected and analyzed for remaining chromate and arsenate concentrations. Amount of anion uptake at equilibrium (q_e value, mg g^{-1}) was calculated from the following equation:

$$q_e = \frac{(C_0 - C_e)V}{m} \quad (1)$$

where, C_0 and C_e are the initial and equilibrium metal ion concentration in aqueous medium (mg L^{-1}), V is volume of the sample (L) and m is the amount of adsorbent added (g). The influence of nanoparticle concentration on the adsorption of arsenate and chromate was performed with a malachite nanoparticle concentration from 5 to 20 g L^{-1}. Adsorption isotherms were studied with varying concentrations of chromate and arsenate (20–500 mg L^{-1}) with fixed amount of malachite nanoparticles (5 g L^{-1}). Temperature depended studies were performed in an increasing temperature range from 10 to 40 °C in an indigenous temperature controlled stirring unit coupled with a water cooler (*Lauda*). Competitive adsorption study of these anions was performed with a mixed solution containing 50 mg L^{-1} of both chromate and arsenate. The adsorption efficiency of each ions was calculated from the following equation,

$$\text{Adsorption efficiency}(\%) = \frac{C_i - C_f}{C_i} \times 100 \quad (2)$$

where C_i and C_f are respective initial and final concentration of chromate and arsenate individually in the mixed system. Desorption of chromate and arsenate from the adsorbent surface was carried out in batch mode. After equilibrium reaches, the adsorbent containing adsorbed chromate and arsenate was separated by centrifugation and air dried. For desorption studies after drying the adsorbent was re-dispersed and the pH was raised from 9 to 12 using 0.1–0.5 M NaOH. The mixture was centrifuged at a regular time interval and the supernatant was measured for the concentration of desorbed chromate and arsenate in liquid phase. Similarly the desorption efficiency of each ions was calculated from the following equation,

$$\text{Desorption efficiency}(\%) = \frac{(C_i - C_f) - C_d}{(C_i - C_f)} \times 100 \quad (3)$$

Here, C_d is the concentration of each ions after desorption from malachite nanoparticle surface. The concentration of total chromium and arsenic was measured in atomic absorption spectrophotometer (*Spectra AA Varian, model 55B*) after adsorption and desorption. Control was taken in each case and all experiments were performed in duplicate for data consistency.

3. Results and discussion

3.1. Influence of solution pH

Surface properties of the adsorbent and ionic forms of metal ions in solution are largely controlled by the initial pH of the medium. The value of pH_{PZC} of malachite nanoparticles is around 7.5. The adsorption efficiency was maximum for pH 4 in both the cases of chromate and arsenate and reduces thereafter as the pH was raised (Fig. 1a). The presence of chromate and arsenate on the malachite nanoparticle surface after adsorption was confirmed by EDX analysis (Fig. 1b and c). These results could be justified taking the pH_{PZC} of the malachite nanoparticle surface into account and the anionic forms of both the anions. In the pH range from 2 to 6, for Cr(VI), $HCrO_4^-$ and $Cr_2O_7^{2-}$ are predominating species in the equilibrium and in basic medium it exist as CrO_4^{2-} [20]. Similarly As (V) ion occurs mainly in the form of H_2AsO_4 – in the pH range between 3 and 6, while a divalent anion $HAsO_4^{2-}$ dominates at higher pH values [21]. Therefore, at pH range 2.0–6.0, the malachite surface ($pH < pH_{PZC}$) remains positively charged and further the –OH groups in the malachite surface gets protonated to a higher extent and turns to $-OH_2^+$. This positively charged malachite surface facilitates the electrostatic interaction [22,23] with the anionic pollutants, which in turn leads to a higher adsorption capacity. At higher pH, due to more OH^- ions on malachite surface carrying net negative charges, the repulsion between the anions (CrO_4^{2-} and $HAsO_4^{2-}$) [24] and the nanoparticles surface increases, which results in a decreased adsorption capacity of both the anions.

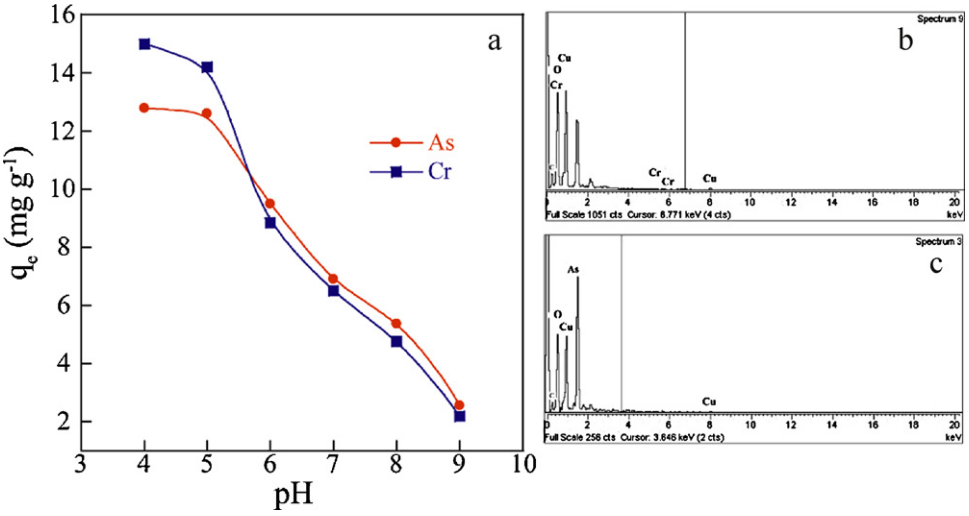

Fig. 1. (a) Effect of initial solution pH on chromate and arsenate ions adsorption by malachite nanoparticles. (Chromate and arsenate concentration = 100 mg L^{-1}; adsorbent dose = 5 g L^{-1}) and EDX analysis of adsorbed (b) arsenate and (c) chromate on malachite nanoparticles.

3.2. Adsorption steady state and kinetic model

The kinetics of adsorption describes the rate of ions uptake on the nanoparticle and this rate controls the equilibrium time. The kinetics of adsorbate uptake is required for selecting optimum operating conditions for the full-scale batch process [25]. The kinetic parameter, which is helpful for the prediction of adsorption rate, gives important information for designing and modeling the processes. Thus, the effect of contact time was analyzed from the kinetic point of view. From the equilibrium studies, it was found that steady state reaches within 12 h and 5 h for chromate and arsenate respectively irrespective of initial concentration (Fig. 2). The adsorption kinetics of chromate and arsenate adsorption on malachite nanoparticle was studied with respect to Lagergren first order (Eq. (4)) and second order kinetic model (Eq. (5)) [26].

$$\log(q_e - q_t) = \log q_e - \left(\frac{1}{2.303}\right) k_1 t \quad (4)$$

$$\left(\frac{t}{q_t}\right) = \left(\frac{1}{q_e^2 k_2}\right) + \left(\frac{t}{q_e}\right) \quad (5)$$

where, the q_t and q_e (mg g^{-1}) are the adsorption capacities at time t and at equilibrium, respectively. k_1 (L min^{-1}) and k_2 (g mg^{-1} min^{-1}) are first and second order rate constant, respectively. Table 1 shows all the kinetic constant values. It was found that the first order rate equation showed correlation coefficient of 0.984 for chromate and 0.990 for arsenate; while the second order correlation coefficient was 0.994 for chromate and 0.995 for arsenate (Table 1). Therefore the adsorption process for both chromate and arsenate can be better described by the second order reaction kinetics.

Another empirically established functional relationship proposed by Weber and Morris [27], the intraparticle diffusion model was applied to fit the kinetic experimental results. The root time dependent equation is given (Eq. (6)) by,

$$q_t = K_i t^{1/2} + C \quad (6)$$

where K_i (mg g^{-1} min$^{-0.5}$) is an intraparticle diffusion rate constant and C (mg g^{-1}) is the intercept. The slope in the linearized fitted curve using intraparticle model (Table 1), characterizes the rate parameter corresponding to the intraparticle diffusion, whereas the intercept of this portion is proportional to the boundary layer thickness. The values of rate constant K_i and C were calculated from the fitted model and given in Table 1. The linearized curve in both the cases do not passes through the origin (~1.0 mg g^{-1} for chromate and ~3.6 mg g^{-1} for arsenate) indicates that intraparticle diffusion is involved in the adsorption process but it is not the only rate-

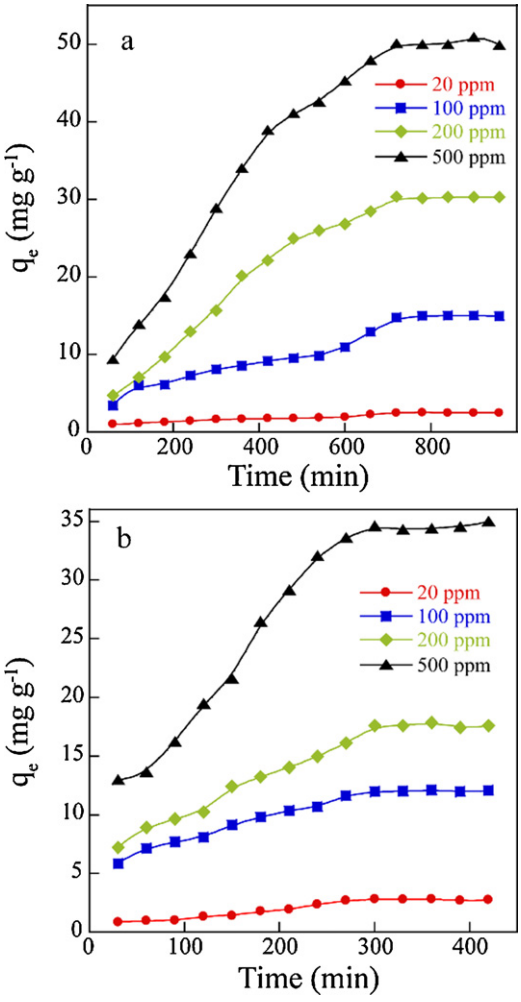

Fig. 2. Effect of initial metal concentration and contact time on adsorption (a) for chromate and (b) for arsenate (pH 5; absorbent dose = 5 g L^{-1}; temperature = 30 ± 1 °C; stirring speed = 200 rpm for both).

Table 1
Comparison of rate constants calculated and q_e values based on respective first-order, second-order and intra-particle diffusion kinetic models.

	q_e exp (mg g^{-1})	First order kinetics			Second order kinetics			Intra-particle diffusion kinetics		
		q_e cal. (mg g^{-1})	k_1 (L min^{-1})	R^2	q_e cal. (mg g^{-1})	k_2 (g mg^{-1} min^{-1})	R^2	K_i (mg g^{-1} min$^{-0.5}$)	C (mg g^{-1})	R^2
Chromate	14.2	11.6	0.0015	0.984	13	0.0004	0.994	0.3950	1.0	0.983
Arsenate	12.5	8.1	0.0071	0.990	14.0	0.0011	0.995	0.4507	3.6	0.982

limiting mechanism and that some other mechanisms also play an important role. Surface adsorption and intraparticle diffusion were likely to take place simultaneously.

3.3. Effect of malachite nanoparticle concentration

Concentration of malachite nanoparticles was varied from 5 to 20 g L^{-1} (for 100 mg L^{-1} initial chromate and arsenate) in a batch mode adsorption study at pH ~5.0. As the concentration of malachite nanoparticle was increased from 5 g L^{-1} to 20 g L^{-1} the adsorption capacity (q_e) was found to decrease (Fig. 3). The total removal efficiency (%) of chromate and arsenate is increased with the increase in malachite nanoparticle concentration. As the mass of the adsorbent is increased, the total surface area and in turns the number of active adsorption sites increases. However the amount of anions adsorbed per unit mass/area of adsorbent decreases, due to the increase in available surface area, resulting in reduction of the adsorption capacity (q_e).

3.4. Effect of initial ion concentration and adsorption isotherm

The equilibrium adsorption isotherm of chromate and arsenate are presented in Fig. 4. The initial anion concentration was varied from 20 to 500 mg L^{-1} with 5 g L^{-1} of malachite nanoparticles at pH ~5.0. According to the slope of initial portion of the curve, as seen from Fig. 4, the adsorption isotherm may be classified as H-type of the Giles' classification [28]. The H-type isotherms are the most common and correspond to high affinity of adsorbate for a given adsorbent. Hence, competition from the solvent for adsorption sites was not observed. As the isotherm tends to plateau, it seems reasonable to assume that complete coverage of the adsorbent surface occurs and steady state is reached.

The adsorption process of chromate and arsenate is analyzed with Langmuir, Freundlich and Dubinin–Radushkevich isotherm model. The main consideration of Langmuir isotherm is sorption takes place at specific homogeneous sites within the adsorbent, indicating a monolayer adsorption process (constant heat of adsorption for all sites). The linearized Langmuir isotherm is expressed as

$$\frac{C_e}{q_e} = \left(\frac{1}{Q_m b}\right) + \left(\frac{1}{Q_m}\right) C_e \quad (7)$$

where, C_e (mg L^{-1}) and q_e (mg g^{-1}) is the equilibrium metal ion concentration in aqueous and solid phase respectively. Q_m is the maximum monolayer uptake by the adsorbent (mg g^{-1}), and b is the Langmuir binding constant of the adsorption. A constant separation factor called "constant separation factor" or "equilibrium parameter", R_L is defined as

$$R_L = \frac{1}{(1 + bC_0)} \quad (8)$$

The values of R_L informs about the favorability of the sorption process. For a favorable adsorption process, $0 < R_L < 1$; whereas $R = 0$ for the irreversible case, $R = 1$ for the linear case and $R > 1$ for unfavorable adsorption process [26]. The Freundlich adsorption isotherm is generally based on multilayer adsorption on heterogeneous surface this holds the assumption that the adsorption sites are distributed exponentially with respect to heat of adsorption. Freundlich isotherm is given as

$$\log q_e = \log K_f + \frac{1}{n} \log C_e \quad (9)$$

K_f (mg g^{-1}) is the Freundlich's uptake factor and n denotes Freundlich's intensity factor [29]. The value of n in the range of 1–10 denotes favorable adsorption, could be find out from the linearized

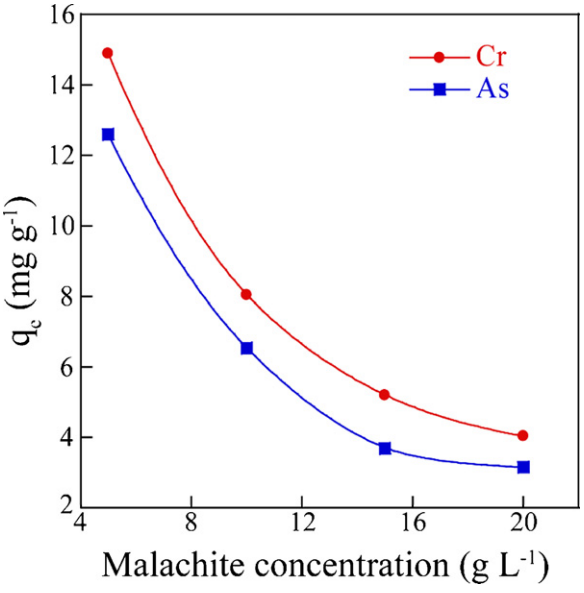

Fig. 3. Effect of nanoparticle concentration on the adsorption of (a) chromate and (b) arsenate (pH 5.0; initial anion concentration = 100 mg L^{-1}; temperature = 30 ± 1 °C; stirring speed = 200 rpm for both).

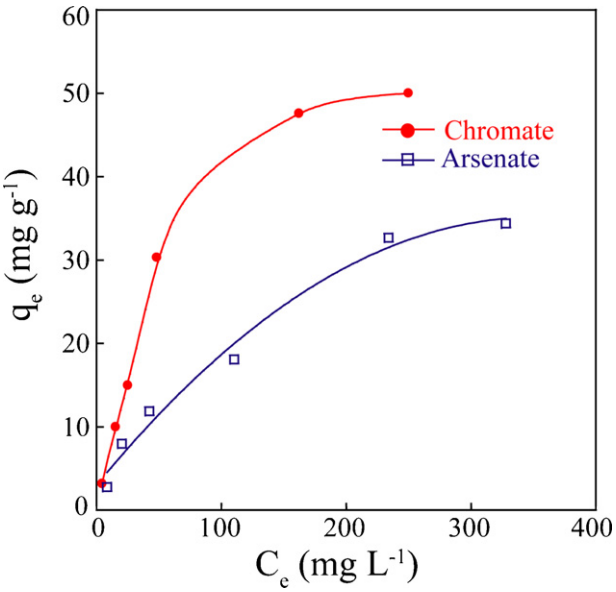

Fig. 4. Adsorption isotherm plot of (a) chromate and (b) arsenate, on malachite nanoparticles (pH 5.0; temperature = 30 ± 1 °C; stirring speed = 200 rpm for both).

Table 2
Adsorption isotherm parameters of chromium and arsenate on malachite nanoparticles.

	Langmuir isotherm				Freundlich isotherm			*D–R* isotherm		
	Q_m (mg g^{-1})	b (L mg^{-1})	R^2	R_L	K_f (mg g^{-1})	n	R^2	Q_0 (mg g^{-1})	K_{DR} (mol^2 kJ^{-2})	R^2
Chromate	82.2	0.009	0.999	0.52	1.472	1.45	0.975	41.07	0.0437	0.931
Arsenate	57.1	0.006	0.992	0.62	1.559	1.85	0.981	25.028	0.0596	0.841

form of Freundlich isotherm. The values of regression coefficients obtained from these models were used as the fitting criteria to find out these isotherms. It was found that the plots in both the cases depicted the linear form of the isotherms and the extremely high correlation coefficients ($R^2_{Langmuir} = 0.999$ for chromate and 0.992 for arsenate; $R^2_{Freundlich} = 0.975$ for chromate and 0.981 for arsenate), indicating both monolayer and heterogeneous surface conditions may exist. The maximum adsorption capacity (Q_m) for chromate and arsenate, obtained from Langmuir isotherm model was 82.2 mg g^{-1} and 57.1 mg g^{-1}, respectively (Table 2). The R_L values, calculated using Eq. (8), were in between 0 and 1 (0.52 and 0.62 for chromate and arsenate respectively) for both the anions, indicating the favorable adsorption process.

Dubinin and Radushkevich (*D–R*) equation [30] is represented in a linear form by equation:

$$\ln q_e = \ln Q_0 - K_{DR}\varepsilon^2 \tag{10}$$

where, K_{DR} (mol^2 kJ^{-2}) is a constant related to mean adsorption energy; and ε is the Polanyi potential, which can be calculated from equation:

$$\varepsilon = RT \ln\left(1 + \frac{1}{C_e}\right) \tag{11}$$

The slope of the plot of $\ln q_e$ versus ε^2 gives K_{DR} (mol^2 kJ^{-2}) and the intercept yields the sorption capacity, Q_0 (mg g^{-1}). T is the absolute temperature in K and R is the universal gas constant (8.314 J mol^{-1} K^{-1}). The adsorption energy for these anions on malachite nanoparticles can be calculated using the following relationship [30],

$$E = \frac{1}{\sqrt{2K_{DR}}} \tag{12}$$

The isotherm constants for Langmuir, Freundlich and D–R models are calculated from the isotherm equations and given in Table 2. The adsorption energy of chromate and arsenate worked out using Eq. (12) was found to be 3.38 kJ mol^{-1} and 2.89 kJ mol^{-1}, respectively. In both the cases the E value is less than 16 kJ mol^{-1}, which indicates that the physical adsorption is the major process involved for adsorption of chromate and arsenate. The positive value of E indicates that the sorption process was endothermic so that higher solution temperature would favor the sorption process.

3.5. Effect of temperature and thermodynamic study

Temperature of the system in an adsorption process is very important regulating parameter which is associated with different thermodynamic aspect of this process. The thermodynamic favorability of a process can be obtained from this analysis. To study the thermodynamics of a process, the adsorption was carried out at different temperature from 10 °C to 40 °C for 100 mg L^{-1} of concentration for both chromate and arsenate. It was found from the results that the adsorption capacity increased from 11.4 mg g^{-1} to 15.6 mg g^{-1} for chromate and 10.1 mg g^{-1} to 12.1 mg g^{-1} in case of arsenate when temperature is increased from 10 °C to 40 °C (Fig. 5a). The standard Gibbs free energy change (ΔG°) was calculated from the following equation,

$$\Delta G^\circ = -RT \ln(K_c) \tag{13}$$

where R is the universal gas constant (8.314 J mol^{-1} K^{-1}) and T is temperature in Kelvin. K_c is the equilibrium stability constant, which was calculated at each temperature using the relation,

$$K_c = \frac{C_s}{C_e} \tag{14}$$

where, C_s and C_e is the equilibrium chromate and arsenate (in respective cases) concentration on adsorbent and aqueous phase, respectively. The Gibbs free energy changes (ΔG°) in this temperature range were calculated from Eq. (13), and are given in Table 3. The negative values of ΔG° suggest that the adsorption process is spontaneous and thermodynamically favorable [31]. The average standard enthalpy change (ΔH°) and entropy (ΔS°) were determined from Van't Hoff equation (Eq. (15)),

$$\ln(K_c) = \left(\frac{\Delta S^0}{R}\right) - \left(\frac{\Delta H^0}{R}\right)\frac{1}{T} \tag{15}$$

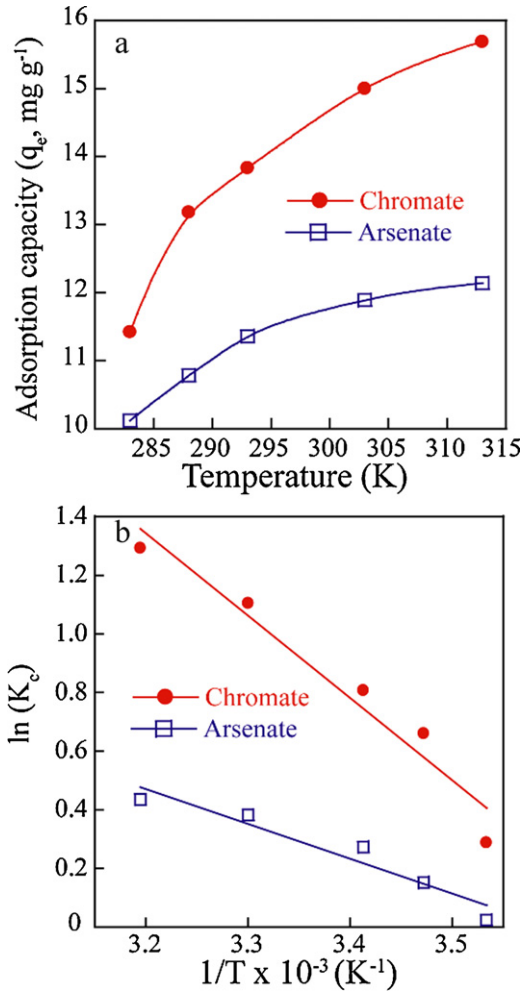

Fig. 5. (a) Adsorption capacity of chromate and arsenate in temperature range of 10–40 °C and (b) Van't Hoff plot of chromate and arsenate adsorption on malachite nanoparticles.

Table 3
Thermodynamic parameters of chromate and arsenate adsorption onto malachite nanoparticles.

Temp. (K)	Chromate			Arsenate		
	ΔG° (kJ mol^{-1})	ΔS° (J mol^{-1} K^{-1})	ΔH° (kJ mol^{-1})	ΔG° (kJ mol^{-1})	ΔS° (J mol^{-1} K^{-1})	ΔH° (kJ mol^{-1})
283	−0.676	85.88	23.34	−0.056	35.47	9.861
288	−1.580			−0.371		
293	−1.966			−0.665		
303	−2.781			−0.963		
313	−3.360			−1.131		

ΔH° and ΔS° was calculated from the slope and intercept of plot between ln (K_c) vs. ($1/T$) based on Van't Hoff equation (Fig. 5b). To a certain extent, physisorption and chemisorption can be classified by the magnitude of the enthalpy change (ΔH°). Bonding strengths of less than 84 kJ mol^{-1} are typically considered as those of physisorption bonds. Chemisorption bond strengths can be 84–420 kJ mol^{-1} [32]. From Van't Hoff curve it was found that the value of ΔH° is about 23.3 and 9.86 kJ mol^{-1} K^{-1}, respectively for chromate and arsenate. This established that in adsorption process takes place mainly through physisorption. This also supports the previous discussion obtained from D–R isotherm model. The value of ΔS° was found to be positive reflecting the spontaneity of the adsorption process. The positive values of ΔH° revealed that the adsorption process was endothermic in nature; which leads to the higher adsorption capacity at higher temperature as obtained from this experiment.

3.6. Competitive adsorption and desorption studies

Competitive study with 50 mg L^{-1} of both chromate and arsenate reflects similar adsorption behaviour as observed in single-component study. The adsorption efficiency of chromate and arsenate from binary mixture was ~70% and ~61%, respectively (Fig. 6a). However in binary mixture, the adsorption efficiency (%) of these two pollutants decreases to some extent compared to that of in single-component study (~75% for chromate and ~66% for arsenate). This is mainly due to the competitive binding of these two anions on malachite nanoparticles.

Moreover, in the competitive and single-component study, the binding capacity of these anions on malachite nanoparticles was analyzed with the respective distribution coefficient (K_d) values of each ions. The distribution coefficient (K_d) is described as the ability of adsorbents to remove a given ion from solution and can be expressed as

$$K_d = \frac{q_e}{C_e} \tag{16}$$

where q_e and C_e are steady-state concentrations of a given ion on adsorbent (mg g^{-1} of adsorbent) and in solution (mg L^{-1}), respectively. The K_d values of chromate (~0.47 L g^{-1}) is slightly higher than that of arsenate (~0.31 L g^{-1}) in both single-component and competitive study (Fig. 6b). However, the K_d values of both the anions decreases in competitive study compared to that in single-component study. In a mixed solution, the decrease in K_d value of an ion is mainly due to the competitive binding of chromate and arsenate present in the solution.

In addition, in a competitive study, the adsorption of different metal ions is mainly governed by the preferential binding affinity of the ions toward the binding site of the adsorbent. A selectivity

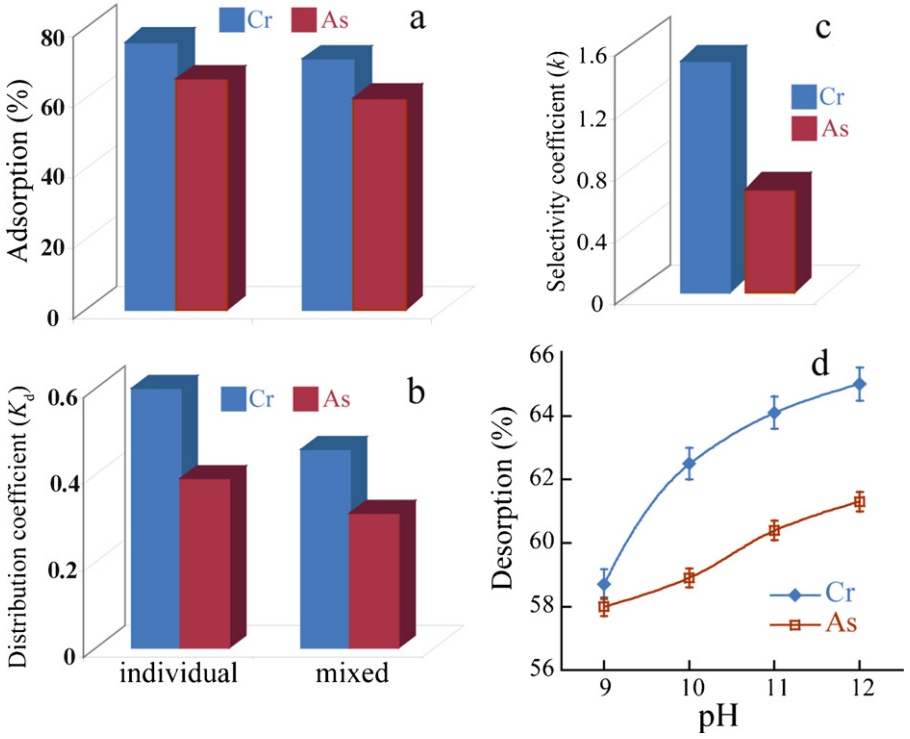

Fig. 6. (a) Adsorption efficiency of chromate and arsenate from a mixed solution containing 50 mg L^{-1} of each anion (at pH ~5.0); (b) distribution coefficient (K_d) values of chromate and arsenate in individual and competitive adsorption process; (c) selectivity coefficient values (K) of chromate and arsenate in a competitive adsorption process; and (d) desorption efficiency of both chromate and arsenate in higher alkaline pH.

coefficient (K) for the binding of a specific ion in the presence of other competitive ions can be obtained from equilibrium binding data (Eq. (17)) [33]

$$m_1(\text{solution}) + m_2(\text{adsorbent}) \rightarrow m_1(\text{adsorbent}) + m_2(\text{solution}) \quad (17)$$

$$K_1 = \frac{\{[m_1]_{\text{adsorbent}}[m_2]_{\text{solution}}\}}{\{[m_1]_{\text{solution}}[m_2]_{\text{adsorbent}}\}} = \frac{K_d(m_1)}{K_d(m_2)} \quad (18)$$

where, K_d is the distribution coefficient of the metal ions and K_1 represents the ratio of K_d values of one ion (m_1) to another (m_2) used in the mixed solution. In the competitive study of chromate and arsenate, the selectivity coefficient of chromate ($K_{Cr/As} = 1.5$) is higher than that of arsenate ($K_{As/Cr} = 0.67$) (Fig. 6c). This indicates a comparatively higher binding affinity of chromate than arsenate, which also reflects in the adsorption efficiency in competitive study (Fig. 6a).

Desorption efficiency of chromate and arsenate loaded malachite nanoparticles in the pH range from 9.0 to 12.0 is shown in (Fig. 6d). It has been observed that ~58% of the adsorbed anions were desorbed at pH ~9.0–10.0. However, upon increasing the pH up to ~12.0, final desorption efficiency was ~61% and ~66% for chromate and arsenate, respectively. The desorption of these anionic pollutants from malachite nanoparticle surface at higher pH is mainly due to the electrostatic repulsion between the anionic pollutants and malachite surface. As discussed before, at pH > 7.5 the malachite nanoparticle surface is negatively charged and the predominant species of chromate and arsenate is CrO_4^{2-} [20] and $HAsO_4^{2-}/AsO_4^{3-}$ [9] in this pH range. Therefore the electrostatic repulsion between the negatively charged malachite nanoparticle surface and anionic pollutants as well as the electrostatic repulsion between these two anionic species on malachite surface lead to desorption of these pollutants from malachite nanoparticle surface.

4. Conclusion

In this article, we have demonstrated the efficient adsorption of toxic arsenate and chromate from wastewater on malachite nanoparticles at pH~4.0–5.0. However the adsorption capacity decreased with the increase in pH. Kinetic models revealed that the adsorption followed second order kinetics. Intraparticle diffusion rate (K_i) indicates that intraparticle diffusion is involved in the adsorption process but it is not the only rate-limiting mechanism and surface adsorption and intraparticle diffusion were likely to take place simultaneously. The adsorption process was well fitted by the Langmuir isotherm with maximum monolayer coverage of 82.2 mg g^{-1} and 57.1 mg g^{-1} for chromate and arsenate, respectively. The positive E values calculated from the D–R model, indicates that the physical adsorption is the major process involved for adsorption of chromate and arsenate and endothermic in nature. The negative ΔG° and positive ΔS° values from thermodynamic analysis also reveals the spontaneity of the adsorption process. Competitive study with a mixed solution showed the efficient and simultaneous adsorption of both chromate and arsenate on malachite nanoparticles. However, the binding affinity of chromate with malachite surface was found comparatively higher than arsenate as calculated from selectivity coefficient analysis. Therefore, the malachite nanoparticles can be used as a potential nano-structured material for efficient removal of toxic pollutants from wastewater.

Acknowledgement

We acknowledge DST (SR/S1/IC-01/2008) and CSIR (01-2235/08/EMR-II), New Delhi India for financial support. JS acknowledges Centre for the Environment and Central Instrumental Facility, IIT Guwahati for providing working facilities.

Appendix A. Supplementary data

Supplementary data associated with this article can be found, in the online version, at doi:10.1016/j.jhazmat.2010.11.036.

References

[1] M.M. Hassan, Arsenic poisoning in Bangladesh: spatial mitigation planning with GIS and public participation, Health Policy 74 (2005) 247–260.
[2] J. Iqbal, H.-J. Kim, J.S. Yang, K. Baek, J.W. Yang, Removal of arsenic from groundwater by micellar-enhanced ultrafiltration (MEUF), Chemosphere 66 (2007) 970–976.
[3] H. Gecol, E. Ergican, A. Fuchs, Molecular level separation of arsenic(V) from water using cationic surfactant micelles and ultrafiltration membrane, J. Membr. Sci. 241 (2004) 105–119.
[4] M. Costa, Potential hazards of hexavalent chromate in our drinking water, Toxicol. Appl. Pharmacol. 188 (2003) 1–5.
[5] G. Bayramoğlu, M.Y. Arica, Adsorption of Cr(VI) onto PEI immobilized acrylate-based magnetic beads: isotherms, kinetics and thermodynamics study, Chem. Eng. J. 139 (2008) 20–28.
[6] C. Raji, T.S. Anirudhan, Batch Cr(VI) removal by polyacrylamide-grafted sawdust: kinetics and thermodynamics, Water Res. 32 (1998) 3772–3780.
[7] A.E. Sikaily, A.E. Nemr, A. Khaled, O. Abdelwehab, Removal of toxic chromium from wastewater using green alga Ulva lactuca and its activated carbon, J. Hazard. Mater. 148 (2007) 216–228.
[8] H. Li, Z. Li, T. Liu, X. Xiao, Z. Peng, L. Deng, A novel technology for biosorption and recovery hexavalent chromium in wastewater by bio-functional magnetic beads, Bioresour. Technol. 99 (2008) 6271–6279.
[9] D. Mohan, C.U. Pittman, Arsenic removal from water/wastewater using adsorbents: a critical review, J. Hazard. Mater. 142 (2007) 1–53.
[10] N.N. Greenwood, A. Earnshaw, Chemistry of Elements, Pergamon Press, Oxford, 1984 (chapter 13).
[11] C.K. Jain, I. Ali, Arsenic: occurrence, toxicity and speciation techniques, Water Res. 34 (2000) 4304–4312.
[12] WHO (World Health Organisation), Environmental Health Criteria, 18, Arsenic, World Health Organisation, Geneva, 1981.
[13] M.D. Kiping, in: J. Lenihan, W.W. Fletcher (Eds.), Arsenic, the Chemical Environment, Environment and Man, 6, Blackie, Glasgow, 1977, pp. 93–110.
[14] N. Kongsricharoern, C. Polprasert, Chromium removal by a bipolar electrochemical precipitation, Water Sci. Technol. 34 (1996) 109–116.
[15] J.C. Seaman, P.M. Bertsch, L. Schwallie, In situ Cr(VI) reduction within coarse-textured, oxide-coated soil and aquifer systems using Fe(II) solutions, Environ. Sci. Technol. 33 (1999) 938–944.
[16] J. Hu, G. Chen, I.M.C. Lo, Removal and recovery of Cr(VI) from wastewater by maghemite nanoparticles, Water Res. 39 (2005) 4528–4536.
[17] S.E. Bailey, T.J. Olin, R.M. Bricka, D.D. Adrian, A review of potentially low-cost sorbents for heavy metals, Water Res. 33 (1999) 2469–2479.
[18] B. Saha, G. Das, Malachite nanoparticle: a new basic hydrophilic surface for pH-controlled adsorption of bovine serum albumin with a high loading capacity, J. Phys. Chem. C 113 (2009) 15667–15675.
[19] B. Saha, S. Chakraborty, G. Das, A rational approach for controlled adsorption of metal ions on bovine serum albumin–malachite bionanocomposite, J. Phys. Chem. C 114 (2010) 9817–9825.
[20] A. Agrawal, C. Pal, K.K. Sahu, Extractive removal of chromium (VI) from industrial waste solution, J. Hazard. Mater. 159 (2008) 458–464.
[21] A.I. Zouboulis, K.A. Kydros, K.A. Matis, Arsenic(III) and arsenic(V) removal from solutions by pyrite fines, Sep. Sci. Technol. 28 (1993) 2449–2463.
[22] M. Uysal, I. Ar, Removal of Cr(VI) from industrial wastewaters by adsorption, part I: determination of optimum condition, J. Hazard. Mater. 149 (2007) 482–491.
[23] M. Dakiky, M. Khamis, A. Manassra, M. Mer'eb, Selective adsorption of chromium(VI) in industrial wastewater using low-cost abundantly available adsorbents, Adv. Environ. Res. 6 (2002) 533–540.
[24] B.M.W.P.K. Amarasinghe, R.A. Williams, Tea waste as a low cost adsorbent for the removal of Cu and Pb from wastewater, Chem. Eng. J. 132 (2007) 299–309.
[25] M.H. Kalavathy, T. Karthikeyan, S. Rajgopal, L.R. Miranda, Kinetic and isotherm studies of Cu(II) adsorption onto H_3PO_4-activated rubber wood sawdust, J. Colloid Interf. Sci. 292 (2005) 354–362.
[26] P.A. Kumar, M. Ray, S. Chakraborty, Hexavalent chromium removal from wastewater using aniline formaldehyde condensate coated silica gel, J. Hazard. Mater. 143 (2007) 24–32.
[27] W.J. Weber, J.C. Morris, Advances in water pollution research: removal of biologically resistant pollutant from waste water by adsorption, in: Proceedings of 1st International Conference on Water Pollution Symposium vol. 2, Pergamon Press, Oxford, 1962, pp. 231–266.
[28] C.H. Giles, T.H. McEvan, S.N. Nakhwa, D. Smith, Studies in adsorption. Part XI. A system of classification of solution adsorption isotherms, and its use in diagnosis of adsorption mechanisms and in measurement of specific surface areas of solids, J. Chem. Soc. 4 (1960) 3973–3993.
[29] T.C. Voice, W.J. Weber, Sorption of hydraulic compounds by sediments, soils and suspended solids-I, theory and background, Water Res. 17 (1983) 1433–1441.

[30] M. Jain, V.K. Garg, K. Kadirvelu, Adsorption of hexavalent chromium from aqueous medium onto carbonaceous adsorbents prepared from waste biomass, J. Environ. Manage. 91 (2010) 949–957.
[31] S. Chen, Q. Yue, B. Gao, X. Xu, Equilibrium and kinetic adsorption study of the adsorptive removal of Cr(VI) using modified wheat residue, J. Colloid Interf. Sci. 349 (2010) 256–264.
[32] C.Y. Kuo, C.H. Wu, J.Y. Wu, Adsorption of direct dyes from aqueous solutions by carbon nanotubes: determination of equilibrium, kinetics and thermodynamics parameters, J. Colloid Interf. Sci. 327 (2008) 308–315.
[33] S. Dai, M.C. Burleigh, Y. Shin, C.C. Morrow, C.E. Barnes, Z. Xue, Imprint coating: a novel synthesis of selective functionalized ordered mesoporous sorbents, Angew. Chem. Int. Ed. 38 (1999) 1235–1239.